

Fabrication and Characterisation of Novel In-Situ Al6061-SiC-Gr Surface Composite Fabricated by Friction Stir Process

Kuldip Kumar Sahu^{#1}, Raj Ballav^{*2}

[#]Research scholar, Department of Production and Industrial Engineering, NIT Jamshedpur
India, PIN – 831014

^{*}Assoc. Professor, Department of Production and Industrial Engineering, NIT Jamshedpur
India, PIN – 831014

¹kksahu.prod@nitjsr.ac.in, ²rballav.prod@nitjsr.ac.in

Abstract — Metal matrix composites (MMCs) hold combined properties of the matrix, i.e., ductility and toughness, along with the high strength and wear resistance property of reinforced ceramic. MMCs have potential applications in the automotive, aeronautical, and aerospace industries. Friction stir processing (FSP) can be used as a solid-state technique for material processing. In the present exertion, FSP has been utilized to diffuse the nanoparticles of a silicon carbide (SiC) ceramic phase and Graphite particles (Gr) as solid lubricants into Al-6061, an in-situ state. SiC and graphite-reinforced MMCs were fabricated using multi-pass FSP into Al-6061 substrate. An array of blind holes along the stir direction is made on the alloy's surface and filled with ceramic particles. FSP was carried out along the groove to produce surface metal matrix composites. Multi-pass processing was carried out for homogeneous dispersion of particles and to remove porosity from the samples. Microhardness tests, Scanning Electron Microscopy, Optical Microscopy, EDX, and X-Ray Diffraction tests were conducted on composite samples. The results indicate an even distribution of 40-50nm size particles of the ceramic phase in the Aluminium matrix after FSP. The surface composite exhibits a 30-40% increase in microhardness (160 HV) and maintains ductility within the processed zone.

Keywords — Ceramics Particles, In-Situ Ceramics Composite, Mechanical behavior, Multipass friction stir processing, Surface metal matrix composites.

I. INTRODUCTION

From the time of the invention of Friction stir welding, several research works have been conducted based on it. Friction Stir Process is one of Friction Stir Welding's derived processes in which surface modification of light metal alloy can easily be done [1-2]. Aluminum AA6061 is a unique and most extensively used aluminum alloy in automobile industries. The heat treatable and can be extruded easily with regular to high strength competencies. The elemental composition of Al-6061 aluminum is shown in table1. Friction stir processing (FSP) can be used as a secondary process to refine grain from fine to ultrafine grain (UFG). During friction stir processing, the stir zone heated up to 60% of the base metal's melting point

temperature and undergoes high plastic deformation (SPD) [3]. This severe plastic deformation and mechanical stirring by tool shoulder lead to grain refinement, thus improving mechanical and metallurgical properties. But in this process, the improvement in hardness and other mechanical properties are not uniform across the friction stir processed (FSPed) zone [4]. High hardness is observed along the thermally mechanically affected zone (TMAZ) with respect to heat affected zone and stir zone. Dispersion of micro or nano-ceramics particles over base metal can improve this uneven distribution of hardness and other mechanical properties across the FSPed zone, i.e., fabricating metal matrix composite. The severe plastic deformation, along with material flow occurring along the stir zone during FSP, can be applied to blend micro or nano-ceramics particles into the stir zone [5]. The homogeneous distribution of reinforcement particles in the stir zone can be confirmed by multiple passes of FSP [5-6]. This process can improve the mechanical and tribological properties of the metal matrix. Numerous strengthening concepts are involved for this enhancement: (1) grain and sub-grain boundary strengthening (Hall-Petch relationship), (2) pinning effect due to restriction in dislocation movement due to presence of reinforcement particles (Orowan theory), (3) dislocations effect due to difference in coefficients of thermal expansion (CTE) of soft matrix and hard reinforcements, and (4) elastic strain in the matrix-reinforcement interface [7].

Previous studies have concluded that reinforcement of ceramic particles can restrict grain growth due to the pinning effect while recrystallization in the FSW/FSP of base metal [8]. Hsu et al. [6] have reported that the existence of finely dispersed Al₃Ti along the stir zone during FSP can restrict grain growth and produces fine grain structure in the matrix metal. A similar result has been reported for FSP of copper alloy with SiC nanoparticles as reinforcement [10]. Therefore, by using FSP of Al sheets with ceramics nanoparticles, grain growth during recrystallization can be restricted, and consequently, mechanical properties of the processed metal can be improved better than the base metal [11].

The present study aims to improve the strength and hardness thus wear resistance of the stirred zone by mixing ceramics particles during FSP of hot rolled and artificially



aged aluminum sheets and also to study the effect on mechanical and microstructural properties by adding solid lubricant as reinforcement particles. For this purpose, Al6061-T6 aluminum sheets are severely deformed by employing many passes. After that, these samples are friction stir processed with and without SiC (40-nanometer average particle size) particles and a mixture of SiC-Gr (in 1:4 volume ratio) particles [12-14]. Further, the influence of multi-pass FSP on the stir zone's microstructure, distribution of SiC nanoparticles, and mechanical properties of the processed samples are discussed.

II. EXPERIMENTAL DETAIL

An easy way to comply with the conference paper formatting requirements is to use this document as a template and simply type your text into it. In this study, FSP has been applied on 5mm-thick Al6061-T6 aluminum sheets for the fabrication of MMC. The chemical composition of Al6061 aluminum has been given in Table 1. Besides, the SiC micro-particles with a diameter in the range of 40-50 μm were used. An array of blind holes was made for the pre-deposition of SiC particles along the base plate's processing direction and filled with the ceramic particles. The volume percentage of powder to make in-situ with aluminum matrix material along the stir zone is approximately 10 – 12%. Table 2 shows the scheme of an experiment for the present study.

TABLE I
Chemical composition of matrix material

Component	Al	M	Si	Fe	Cu	Zn	Ti	Mn	Cr
Amount (Wt %)	Balance	0.8-1.2	0.4 – 0.8	Max. 0.7	0.15-0.40	Max. 0.25	Max. 0.15	Max. 0.15	0.04-0.35

TABLE II
Details of experiments and process parameters

Sl. No.	Sample	No. of pass	Rotational speed(rpm)	Traverse speed (mm/min)	Plunge depth(mm)	Tilt angle (°)
1	Al6061	1	1600	25	0.15	2
2		2	1600	25	0.15	2
3		3	1600	25	0.15	2
4	Al6061 +10%SiC	1	1600	25	0.15	2
5		2	1600	25	0.15	2
6		3	1600	25	0.15	2
7	Al6061 +10%SiC	1	1600	25	0.15	2
8		2	1600	25	0.15	2
9		3	1600	25	0.15	2

The values of processing parameters such as rotation speed, traverse speed, plunge depth, and tilt angle were fixed based on the trial experiments and literature survey fixed to 1600 rpm, 25 mm/min, .15 mm 2°, irrespectively. The present study focuses on the fabrication of a new in-situ surface composite and the effect of no. of passes on FSPed MMC properties.

The schematic diagram of the process has been shown in Fig. 1. FSP was performed first by a pin-free tool (Fig. 1(b)) to prevent the spilling out of SiC nanoparticles from the packets and then by a tool with a pin (Fig. 1(c)) to disperse nanoparticles in the aluminum matrix. The pin of the tool has a square cross-section of 5 mm side and 4 mm in height. The tool has a flat shoulder of diameter, and a tilt angle was 20 mm and 2° respectively in the process.

Moreover, the traverse speed and rotation speeds were 25 mm/min and 1600 rpm, respectively. Each sample was FSPed for three no. of passes. After each pass, one sample was cut by using a wire electric discharge machining (Electronica, Maxicut 523) for hardness test and optical microstructure test. X-ray diffraction pattern data of three samples, i.e., alloy without reinforcement, alloy with SiC reinforcement, and alloy with a mixture of SiC and graphite reinforcement, all after three passes of FSP, were taken using an Ultima IV X-ray diffractometer equipped with CuK radiation and Ni filter. The XRD analysis was carried out at a voltage and current rating of 40 kV and 30 mA, respectively. The scanning range was fixed to 20° to 100° with a scanning rate of 0.05 per step.

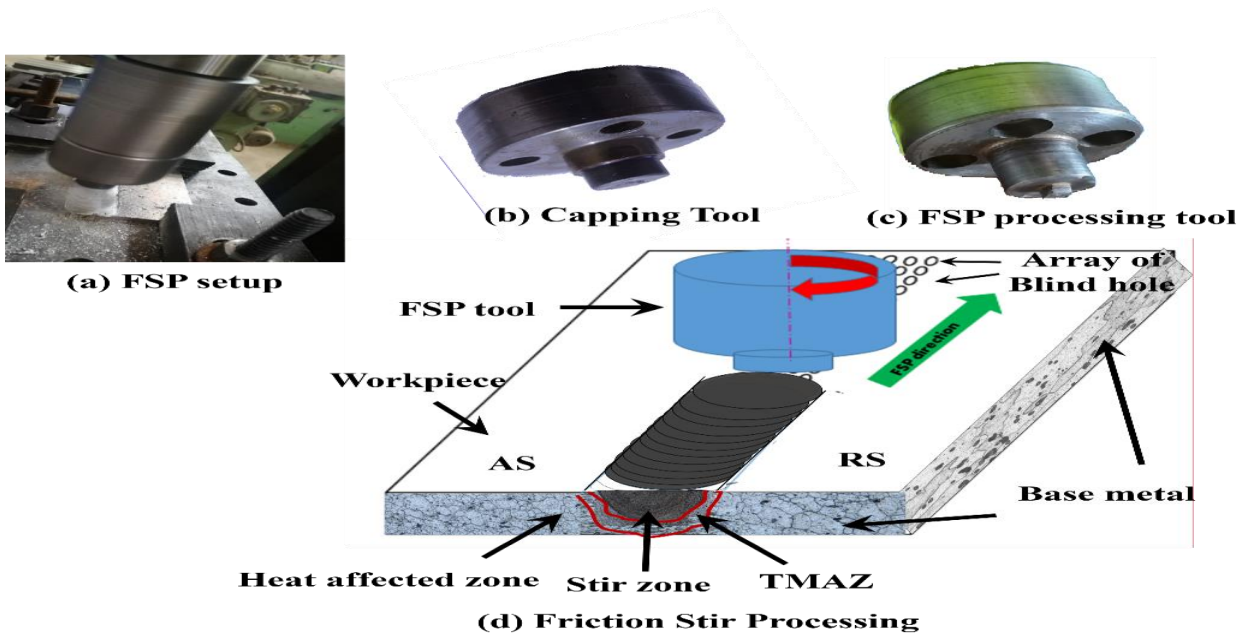


Fig.1 Schematic of the MMC fabrication by the FSP technique (a) capping pass (b) capping tool (c) FSP tool (d) FSP filling passes (conducting multiple FSP passes)

The microstructure of the stirred zone was characterized by using an optical microscope (OM) (Leica, DLM 13). The spreading of SiC nanoparticles was investigated by both OM and scanning electron microscopy (SEM) (ZEISS, EVO 18). To investigate the mechanical behavior of FSPed specimens, uniaxial tensile and Vickers microhardness tests have been carried along the centreline of the cross-section and perpendicular to the FSP direction. The microhardness test was performed with a load of 200 g and a loading period of 15 s by using a micro-hardness indenter (UHL VMHT001). An X-ray diffraction test was conducted for all the samples after three passes.

III. RESULT AND DISCUSSION

Processed samples were prepared as per the scheme of experiments. Test samples from each workpiece are cut and prepared for several tests as per specification. Samples were cleaned and coded before various tests. Following tests has been conducted on samples, and results are discussed in forthcoming sections:

A. Microstructural Study

Microstructural studies of different samples were studied using an optical microscope. Optical images of different significant sites of different samples were examined and compared with each other. Mainly stir zone (SZ), Heat affected zones (HAZ), Thermally Mechanically Affected Zone (TMAZ), and unaffected zones.

a) The microstructure of the base metal and processed zone: The microstructure of different zones of an FSPed sample of Al-6061 has been shown in Fig. 2. As received Al-6061-T6 plate has elongated coarse gain structures (Fig 2(a)) because it is hot rolled and solution heat treated. The average grain size was found as 80-100 μm for the unaltered base metal. The grain size distribution across different zones of the FSPed specimen can be seen in Fig.2.

It can be seen FSP modified the grain structures on the processed zone as compared to the BM. Referring to Fig. 2(b), equiaxed and finer grains have been found in the stir zone (SZ). Material deformation and heat generation due to friction and high strain in the process introduced very high dislocation density at the early stage of deformation leading to the cell formation at the interior of the grains. This phenomenon causes the formation of the Ultra-fine grain (UFG) structure in the SZ. Heat affected zone (HAZ) and thermally affected zone (TMAZ) have relatively coarser grain (Fig. 2(c)) but deformed and elongated grains were observed as shown in Fig. 2(c)-(d). Therefore fine microstructures have been observed in the SZ as compared to the other weld regions due to severe mechanical deformation induced by the FSP tool. Grain size is also dependent on the number of passes. The number of FSP passes increases material deformation and frictional heat on the processed zone.

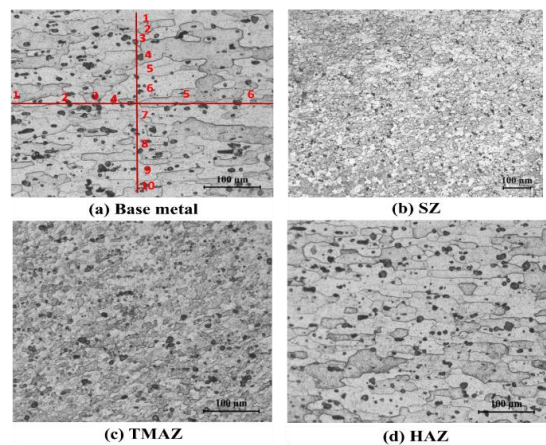


Fig. 2 Microstructures of FSPed Al-6061-T6 without any reinforcement (a) Base material (b) SZ (c) TMAZ (d) HAZ

However, due to the high stacking fault of aluminum, dynamic recrystallizations have occurred, leading to the inhalation of dislocations in the lattice structure and form recrystallized grain [14]. Later in the annealing stage of the FSP, the growth of recrystallized grains has occurred. The grain growth is dependent on frictional. Therefore high material distortion and frictional heat generation in three pass FSP is the likely reason behind the coarsening of grains.

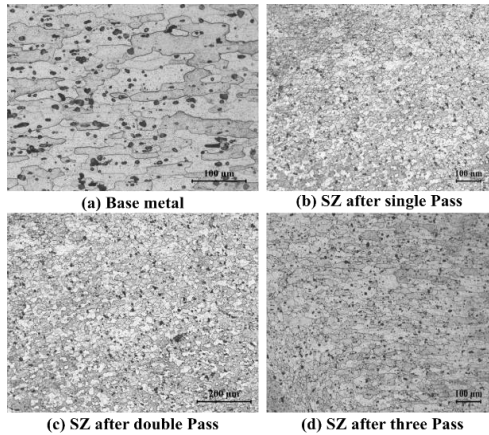


Fig. 3: Microstructures of FSPed specimen without any reinforcement after (a) 1 pass (b) 2 pass (c) 3 pass FSPed of Al6061 with SiC particles

b) The microstructure of the stir zone: Fig. 4 shows the distribution of SiC Ceramics particles in the SZ. It can be seen that the non-uniform distribution of SiC was found on the FSPed cross-section. The reinforcement particles were more homogeneously dispersed at AS than that at RS. This is because of the fact that thermo-mechanical action of

FSP where the plasticized material is forced to flow in a vortex motion from the AS to the RS during FSP [15]. For single-pass FSPed specimens, agglomeration of SiC particles has been found. However, as the number of passes increases from single to triple, the size of SiC powders' aggregation was decreased. This can be explained by the better material mixing in the material caused due to an increase in the number of passes in FSP. In the processes, the FSP tool produces deformation at a high strain rate, which breaks the oxide layer of the matrix as well as SiC, which helps to produce the plasticized material under the effect of frictional heat. Later, further stirring action of the tool during FSP produce stirring of plasticized material in the SZ [16]. However, due to the higher density and softening temperature of SiC particles than the base aluminum, agglomeration of reinforcement particles (SiC) has been observed in a single pass FSP. Besides, thermo-mechanical action of single-pass FSP was insufficient to produce atomic diffusion among the SiC particles and Aluminum matrix, which leads to the formation of cavities and defects, as shown in Fig. 4(a) and 4(b)[16-17]. As the number of passes increases from a single pass, the degree of material mixing and frictional heat increases in the FSPed zones, which helped to produce better diffusion bonding among Al-matrix and SiC. As a result, defect-free MMC was obtained in three pass FSP (Fig. 4(b)-(c)). In addition to that, three passes FSP also yielded near homogenous distribution of SiC particles in the SZ at double and triple passes of FSP, which can be verified from the observation shown in Fig. 4(e)-(f).

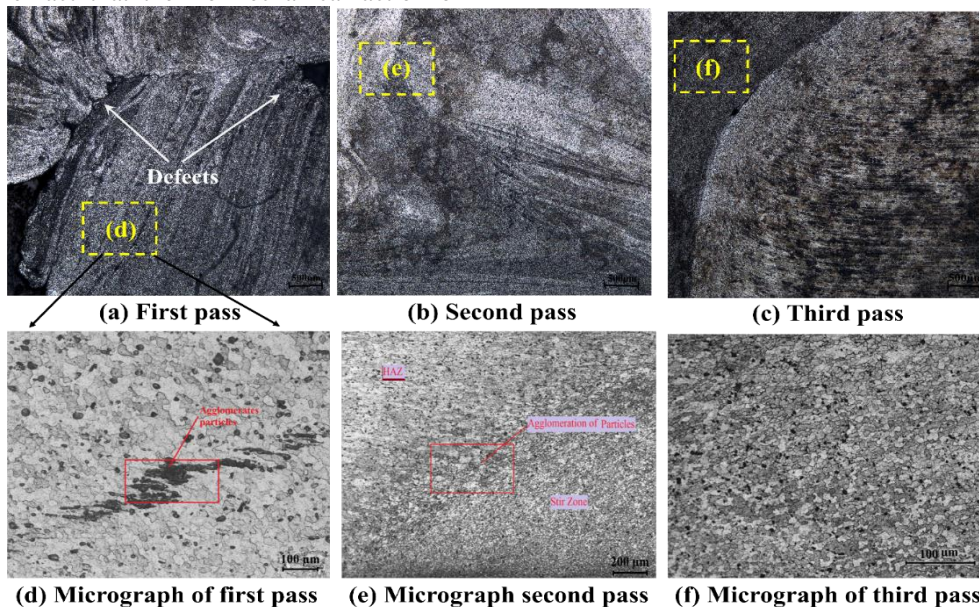


Fig. 4: Optical images of FSPed samples of Al6061- SiC surface composites (a) OM image after one pass (b) OM image after two passes (c) OM image after three pass

While Comparing grain size of FSPed alloy after two-pass (Fig. 3(b)) with that of FSPed surface composite after two-pass (Fig. 4(b)), it is observed that by using SiC nanoparticles, the average grain size of the processed zone

is greatly decreased from 18 μm to approximately 6 μm. Similarly, the grain size of three passes FSPed alloy has an average grain size of 10 μm, which decreases to 3 μm while processed with reinforcement of SiC with three

passes of FSP, mainly in the regions in which these particles are uniformly dispersed. Due to the presence of accumulated coarse SiC in the stir zone, grains of various sizes were formed in a single pass FSPed specimen (Fig. 4(a)) [18]. The average grain size of $4\mu\text{m}$ to $13\mu\text{m}$ can be observed in regions with a cluster of particles and nearly even distributed sites, respectively. Fig. 5(a) indicates the sites with the uneven distribution of reinforcement particles in samples processed with single-pass FSP. Also, Fig. 5(b) is an SEM image of the part of the processed zone where even distribution of ceramic SiC particles has been achieved. It can be observed that finer grains have

been formed in samples processed with 2 pass FSP than that of single-pass FSP. Although the near-uniform distribution of particles can be concluded in 2 pass specimens than that of single-pass specimens with wider sites. It also is noted that the size of sites in which near-uniform distribution of ceramic particles can be seen has increased in 2nd pass with respect to a single pass. This might be the result of successive grain refinement and multiple stirring effects during 2nd pass of FSP due to more plastic deformation and more heat generation due to friction.

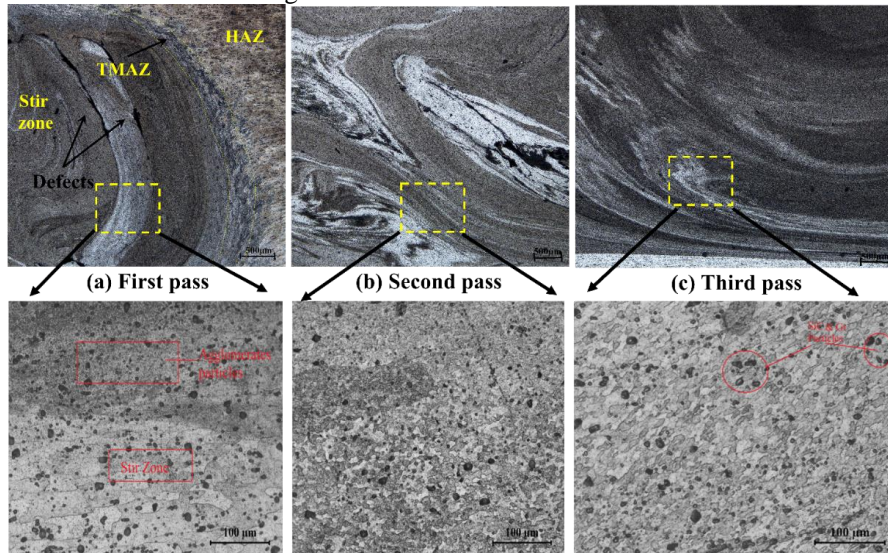


Fig. 5 Optical Microscopy images of Al-SiC- Gr (a) after 1 pass (b) after two passes (c) after three pass

Thus, the effect of an increase in FSP pass can be concluded in the following three points: (1) Plastic (2) Retardation of grain growth due to the presence of widely dispersed and broken ceramics particles. [18], and (3) grain refinement due to the presence of more residual stress in the processed zone. Further, the 3rd FSP pass can shatter the clustered SiC particles, thus greatly retards grain growth. Again, secondary grain growth has been restricted by dispersed and broken ceramic particles in the process zone due to the stirring effect of the tool. Therefore, as discussed in the earlier section, the size of uniformly

deformation of the larger area due to exposure of larger friction heat results in a wider processed zone [19-20], distributed sites of processed zone continuously increases with an increase in the past number of FSP. Also, grains become finer and finer due to the even distribution of reinforcement particles in the processed zone. Comparatively, the stir zone's microstructure for the specimen that has undergone three passes of FSP is relatively more uniform with a smaller grain size than that of 1 and 2 pass FSPed samples.

B. SEM Images of FSPed samples

Fig. 6 (a), 6(b), and 6(c) show the scanning electron micrographs FSPed samples of Al6061 alloy without any reinforcement. It is clearly visualized that there is more porosity in the 1st pass of FSP and can be eliminated after subsequent passes. Similarly, in the case of Al6061 –

SiC surface composite, there are chances of higher porosity and clustering of particles in 1st pass or capping pass of FSP (Fig. 7(a)). By increasing the number of FSP pass, uniform distribution of ceramics powder and decrease in porosity can be observed clearly.

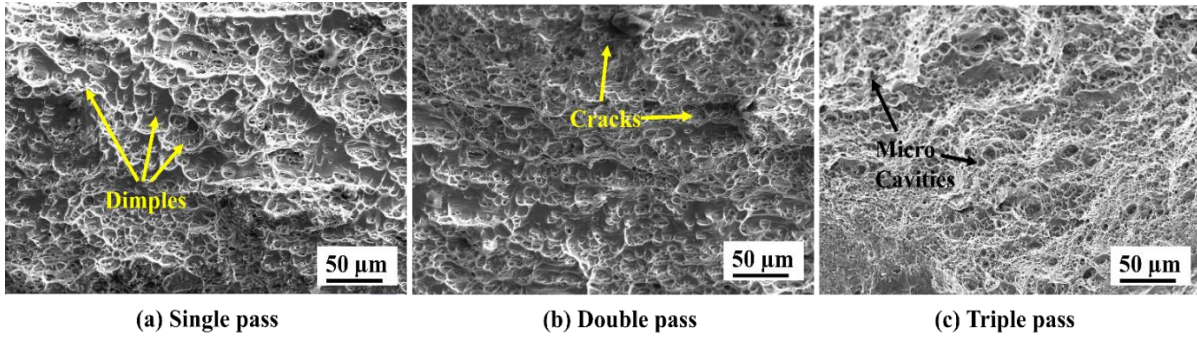


Fig. 6: SEM images of FSPed samples of Al6061 alloy after (a) 1 pass (b) 2 pass (c) 3 pass

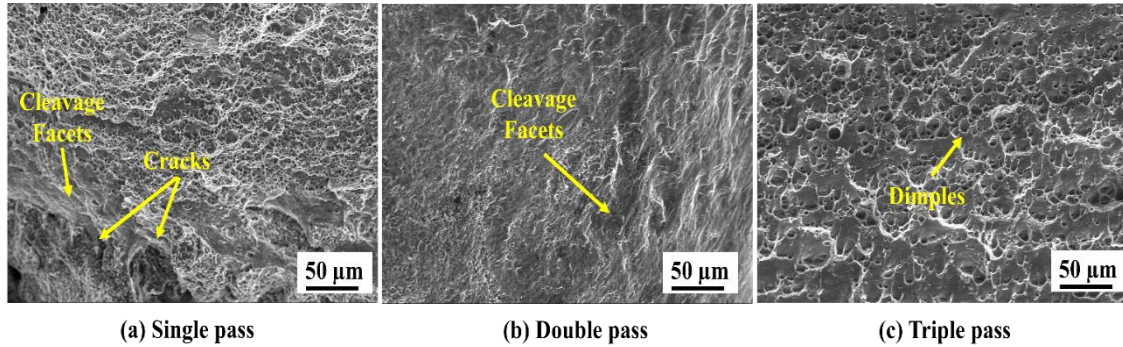


Fig. 7 SEM images of FSPed samples of Al6061 – 10% SiC Surface Composite after (a) 1 pass (b) 2 pass (c) 3 pass

The SEM image of the sample after capping pass is shown in fig. 8(a). The way of powder deposition, i.e., an array of blind holes of 2mm diameter, can be seen in the figure. Also, encapsulate reinforcement powder in the blind hole is visible. In case of Hybrid Composite (Al6061-10% (SiC+ Gr)), the SEM micrographs is shown in figs 8(b) , 8(c) and 8(d). SEM image 8(a) shows the

poor distribution of ceramics particles to the substrate of Al6061. Also, the agglomeration of powders can be easily seen in fig—8 (a). A consecutive number of passes eliminates the accumulation of particles and gives a near approximate homogeneous distribution of powders within the stir zone, which can be seen in figs 8(c) and 8(d).

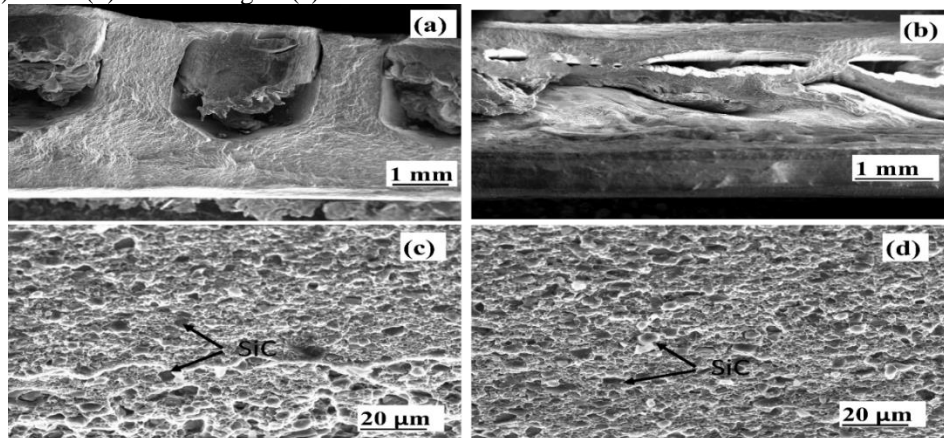


Fig. 8 SEM images of FSPed samples of Al6061 – 10% (SiC + Gr) Surface Composite) a)cross-section after capping pass b) after 1 pass c) after 2 pass d) after 3 passes of FSP

C. EDS test of hybrid surface composite

The elemental mapping in the hybrid surface metal matrix composite in the processed zone can be justified by the EDS test at different spots shown in Figure 9. Three random spots were chosen for the elemental mapping, and thus obtained result is represented. The extracted result shows that all possible elements exist in all three spots. As can be depicted from spot 1, the region rich in SiC Particle

thus higher percent of carbon and Silicon can be observed [21]. At spot 2 maximum amount of aluminum can be observed. Similarly, at spot 3, all possible elements can be observed in respective ratios. All these details show that, due to the processing, a near homogeneous surface hybrid metal matrix composite has been fabricated, and thus, formed composite possesses all possible elements.

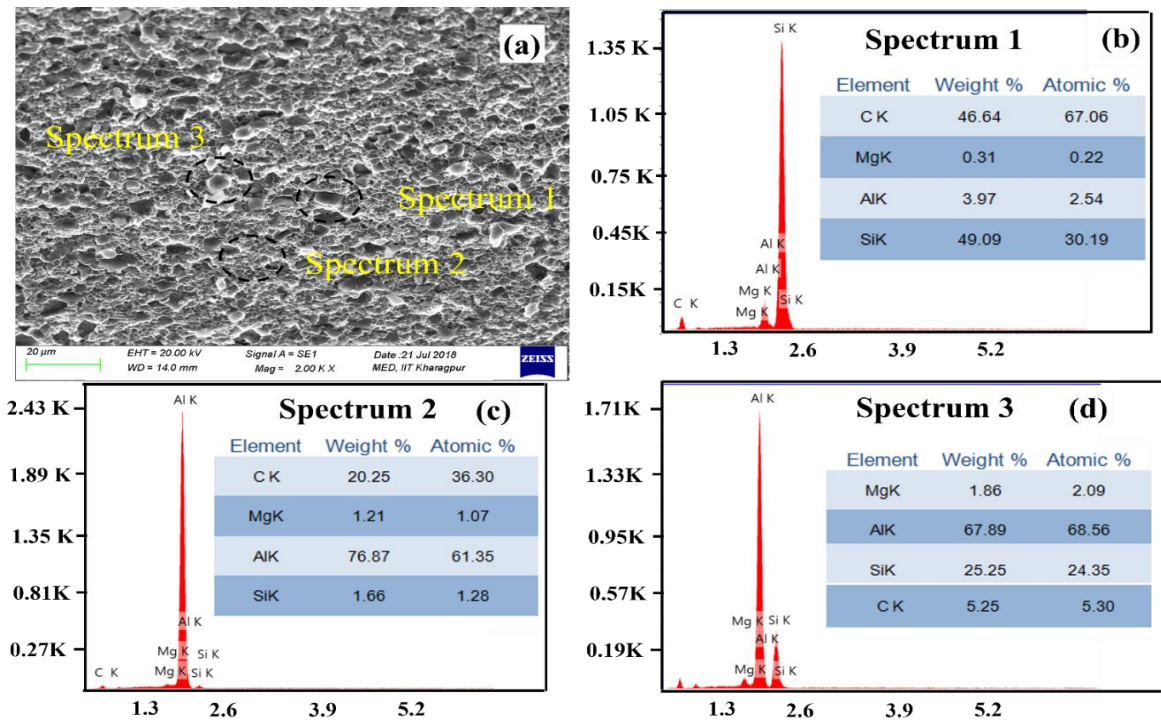


Fig. 9 Elemental mapping by EDS test of Surface Hybrid composite

D. Mechanical properties of FSPed Samples

Processed samples were prepared for mechanical tests such as the uniaxial tensile test and Vicker's microhardness test as per the standard procedure.

a) Microhardness test: Multiple no. of passes during FSP can result from a rise in the surface microhardness of processed Al6061 sheet from 85Hv at the full annealed condition to 115 HV after FSP. The microhardness values for stir zone of FSPed specimens subjected to various FSP pass at three cases: (i) using SiC nanoparticles, (ii) Mixture of SiC particles and graphite particles, and (iii) without any reinforcement are indicated in Fig. 10. It can be observed that samples without SiC particles and that have

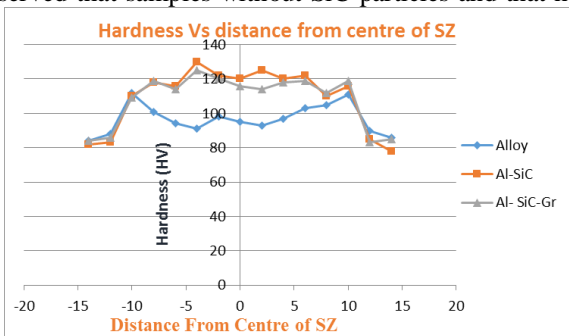


Fig 10: Hardness values across stir Zone of the different element after 3 passes.

Here, SiC particles as reinforcement particles in Al-6061 substrate were used during FSP, which results in retardation of grain growth. The effect of the number of passes of FSP on the mechanical properties of fabricated samples has been studied. Although, even distribution of reinforcement particles can be observed in limited areas,

undergone multiple FSP pass the stir zone's microhardness values are almost the same and greater than that of as-received base metal and about 36% more. Dynamic crystallization thus restricted grain growth is the main reason behind this effect in FSPed samples, as explained in Section 3.1.2. As received plates are hot rolled and solution hardened, so the least residual strain is contained in plates. As a result, FSPed aluminum sheets are found to be unstable upon thermo-mechanical effect, thus affects the grain growth. The combined effect of all these phenomena gives similar results as explained in Section 3.1.2. It should be noted that similar conclusions have been given for FSW of ARBed [22-25] and CGPed [26,27] aluminum base metal sheets.

and this area has been increased with an increase in the number of FSP pass. Finally, 3rd number of the pass can be stated as the optimum pass number for the proposed processing condition. Average microhardness values were measured for three passes of all three samples, i.e., FSPed alloy, SiC reinforced binary MMC, and SiC + Gr reinforced hybrid MMC. FSPed samples have an average hardness improvement of 55% with respect to an unprocessed base metal, whereas SiC reinforced binary composite shows improvement in hardness by 75% that of base metal. Of course, the addition of soft solid lubricants, i. e. graphite particles, shows the decrease in microhardness value of the processed zone, and it shows improvement in hardness by 68 % that of base metal. There is not much effect of pass number in only FSPed alloy because the same phenomena occur in every FSP pass. But in the case of binary composite and hybrid composite, the effect of multipass can be visualized from evenly particle distributed sites, thus an improvement in

average microhardness number with an increase in pass number.

b) Tensile tests of samples: Processed samples were prepared for the unidirectional tensile test as per ASTM E8 standard. Tensile samples were cut transversely with respect to the processed direction. The tensile result of base metal (AL-6061-T6) shows that the hot rolled and age hardened sample behaves like a ductile material having elongation approx 14% before fracture. While base metal has been processed with multipass FSP, a significant change in ductility, as well as ultimate tensile strength, was observed, as shown in Fig 10(a). due to dynamic recrystallization, grain refinement takes place, thus improves the mechanical property such as tensile yield strength and ultimate strength, whereas little decrement in elongation can be depicted from the result [28-30].

When base metal with SiC nanoparticles was processed to get surface MMC using an array of holes for the pre-deposition of powders, a great enhancement in unidirectional tensile strength was observed. The results can be attributed due to the combined effect of dynamic recrystallization and pinning effect. A schematic illustration of the pinning effect has been shown in Fig 11 (b). Due to dynamic recrystallization, fine grains will form in the stir zone, whereas due to the pinning effect, the reinforcement particle creates hindrance in dislocation

movement, thus increases the tensile strength of the component. Same time, if there is an insufficient fusion between two grains during FSP (such case can be seen in single or two passes, which are illustrated in Fig11 (a)), lower tensile strength can be observed in single and two passes. Fig. 10 (b) shows the tensile result of binary surface composite i. e. The al-6061 base metal is reinforced with SiC nanoparticles [31-32]. The presence of defects like the oxide layer between the two gains leads to poor diffusion of grains. Thus, early failure of sample processes with single and double passes takes place.

The soft nature of graphite as a solid lubricant descends the ultimate tensile strength of samples when they are processed with a calculated mixture of Sic and graphite particles. Similarly, early failure of samples processed with single and double passes took place due to the same reason explained earlier. The tensile result of the hybrid surface metal matrix composite is shown in Fig. 10(c). The comparative results of all triple passed surface composites and alloys have been shown in Fig. 10(d).

A relative comparison of ultimate tensile strength, yield tensile strength, and elongation has been shown in Fig. 12. Maximum ultimate tensile strength and yield tensile strength have been observed in 3rd pass binary surface composite, whereas maximum ductility was found in base metal in as-received condition [33].

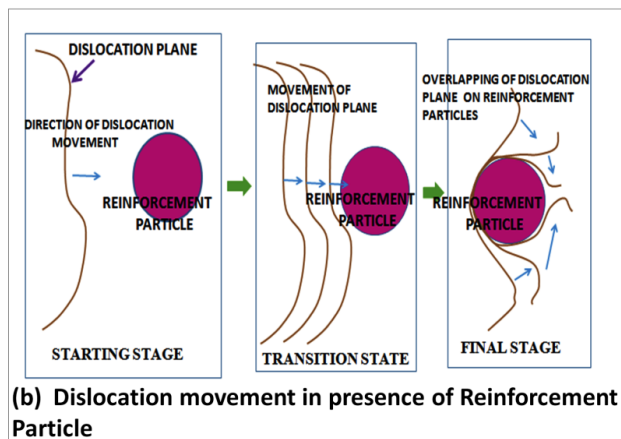
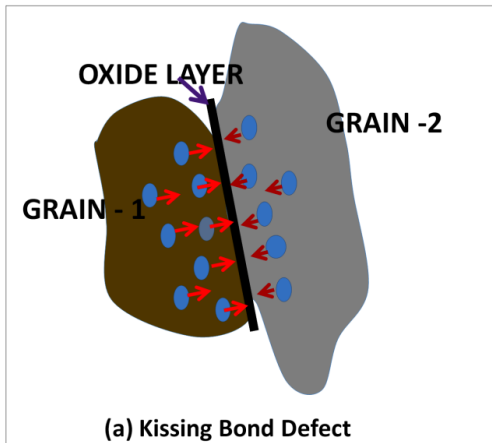


Fig 11 Kissing bond defect and pinning effect

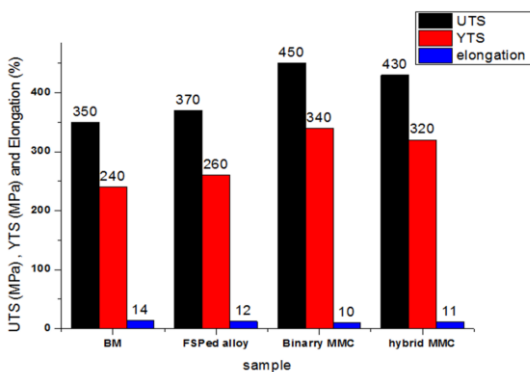


Fig. 12 Ultimate tensile strength, yield tensile strength, and elongation of samples

E. XRD analysis of FSPed Samples

The X-ray diffraction patterns of 3 pass FSP processed specimen no. 9 (i.e., Al6061 + SiC+ Gr, 3 Pass Surface Composite) are depicted in Fig.6. The corresponding diffractogram of the FSPed of Al6061 alloy shows the different phases of different elements present in the material. Accordingly, it may be concluded that a dynamic dissolution process has been taken place in the course FSP. There is evidence of the presence of different phases of oxides of aluminum and other elements.

In the diffractogram for the FSPed sample of surface composite, some peaks are present, which shows the presence of Silicon and silicon carbide (SiC). This provides the reason behind the improvement in the microhardness value of the stir zone. The XRD analysis of

the third sample (hybrid composite) containing mixtures of SiC and Graphite shows evidence of few peaks of the graphite phase. Thus, the third sample's microhardness after the third pass has a lower value of tensile strength

than the second specimen (binary composite), which is only having SiC as reinforcement particles [33-36].

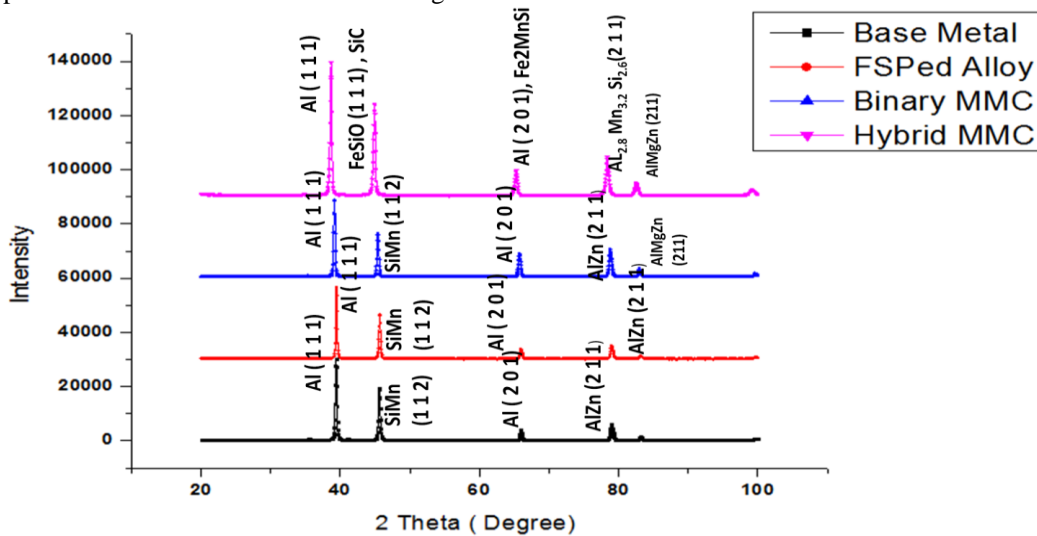


Fig 13: XRD pattern of three specimens after three passes of FSP.

F. Conclusions

Fabrication of SiC-Gr reinforced Al-6061 based hybrid surfaced composite was successfully done using Friction stir processing. Several tests on fabricated samples were conducted, such as microhardness, tensile, optical microscopy, SEM, XRD, and EDS, as per the specified methods. The main conclusions that can be found from this study are

(1) Friction stir processing methodology can be utilized as a new technique of grain refining, thus an improvement in mechanical, tribological, and metallurgical properties.

(2) There is not much difference in the stir zone's microstructure evolution by increasing the FSP pass number of Al-alloy without reinforcing ceramics powders. However, mechanical properties of processed samples, i.e., Al-6061 substrate with SiC particles and a Mixture of SiC and Graphite particles, are greatly affected by the process parameters.

(3) Making an array of holes and filling it with ceramics powder along stir direction before FSP can be used as fabricating method of surface MMC but need to optimize FSP pass number. For the present case, three passes of FSP have been suggested for the fabrication of surface composite.

(4) Clustering of reinforced particles can be observed in the retreating side of the stir zone due to the nature of material flow in FSP. This phenomenon is more in the case of the 1st pass of FSP and continuously reduces with an increase in FSP pass. This clustering of reinforcement particles leads to brittle fracture during the tensile test, and it can be visualized in the case of samples processed with one and two passes of FSP. Weather, failure mechanism shifted to brittle fracture in case of tensile test of sample processed with three FSP pass, and no stress concentration was observed.

(5) A significant improvement in microhardness value (approx 165%) was observed in the case of surface MMC reinforced with SiC particles, whereas 155% improvement in same has been observed in case of hybrid composite reinforced with SiC and Graphite with respect to base metal Al-6061-T6 alloy.

As future work, the dry sliding wear test and corrosion behavior test of such hybrid composite can be done as future work. The FSP process also gives metallurgists and scientists freedom to design various compositions of surface hybrid composites and their characterization.

References

- [1] M. Azizieh, A. H. Kokabi, and P. Abachi., Effect of rotational speed and probe profile on microstructure and hardness of AZ31/Al₂O₃ nano-composites fabricated by friction stir processing., *Materials & Design* 32(4)(2011) 2034-2041.
- [2] C. J. Hsu, et al., Al-Al 3 Ti nano-composites produced in situ by friction stir processing., *Acta Materialia*, 54(19)(2006) 5241-5249.
- [3] A. Shafiei-Zarghani, S. F. Kashani-Bozorg, and A. Zarei-Hanzaki., Microstructures and mechanical properties of Al/Al₂O₃ surface nano-composite layer produced by friction stir processing., *Materials Science and Engineering: A* 500(1)(2009) 84-91.
- [4] Y. Mazaheri, F. Karimzadeh, and M. H. Enayati., A novel technique for the development of A356/Al₂O₃ surface nano-composite by friction stir processing., *Journal of Materials Processing Technology* 211(10)(2011) 1614-1619.
- [5] Ghader Faraji, and Parviz Asadi., Characterization of AZ91/alumina nano-composite produced by FSP., *Materials Science and Engineering*: 528(6)(2011) 2431-2440.
- [6] M. Sarkari Khorrami, M. Kazeminezhad, and A. H. Kokabi. The effect of SiC nanoparticles on the friction stir processing of severely deformed aluminum., *Materials Science and Engineering: A* 602(2014) 110-118.
- [7] Ranjit Bauri et al., Effect of process parameters and tool geometry on the fabrication of Ni particles reinforced 5083 Al composite by friction stir processing., *Materials Today: Proceedings* 2(2015) 4-5 3203-3211.
- [8] S. Sahraeinejad, et al., Fabrication of metal matrix composites by friction stir processing with different particles and processing

- parameters., *Materials Science and Engineering: A* 626 (2015) 505-513.
- [9] Akiko Tajiri, et al., Effect of friction stir processing conditions on fatigue behavior and texture development in A356-T6 cast aluminum alloy., *International Journal of Fatigue* 80(2015) 192-202.
- [10] Helena Polezhayeva, et al., Fatigue performance of friction stir welded marine grade steel., *International Journal of Fatigue* 81(2015) 162-170.
- [11] Siavash Gholami, et al., Friction stir processing of 7075 Al alloy and subsequent aging treatment., *Transactions of Nonferrous Metals Society of China* 25(9)(2015) 2847-2855.
- [12] Ajay Kumar, Rishi Raj, and Satish V. Kailas., A novel in-situ polymer derived nano-ceramic MMC by friction stir processing., *Materials & Design* 85(2015) 626-634.
- [13] F. Khodabakhshi, et al., Effects of nanometric inclusions on the microstructural characteristics and strengthening of a friction-stir processed aluminum-magnesium alloy., *Materials Science and Engineering: A* 642(2015) 215-229.
- [14] Jicheng Gao, et al., Improvements of mechanical properties in dissimilar joints of HDPE and ABS via carbon nanotubes during friction stir welding process., *Materials & Design* 86(2015) 289-296.
- [15] Genghua Cao, et al., Superplastic behavior and microstructure evolution of a fine-grained Mg–Y–Nd alloy processed by submerged friction stir processing., *Materials Science and Engineering: A* 642(2015) 157-166.
- [16] M. Ashjari, A. Mostafapour Asl, and S. Rouhi., Experimental investigation on the effect of process environment on the mechanical properties of AA5083/Al₂O₃ nano-composite fabricated via friction stir processing., *Materials Science and Engineering: A* 645 (2015) 40-46.
- [17] M. Sarkari Khorrami, M. Kazeminezhad, and A. H. Kokabi. "Thermal stability of aluminum after friction stir processing with SiC nanoparticles., *Materials & Design* 80(2015) 41-50.
- [18] Hiroyasu Tanigawa et al., Modification of vacuum plasma sprayed tungsten coating on reduced activation ferritic/martensitic steels by friction stir processing., *Fusion Engineering and Design* 98(2015) 2080-2084.
- [19] M. Sarkari Khorrami, et al., In-situ aluminum matrix composite produced by friction stir processing using FE particles., *Materials Science and Engineering: A* 641(2015) 380-390.
- [20] A. Hamdollahzadeh, et al., Microstructure evolutions and mechanical properties of nano-SiC-fortified AA7075 friction stir weldment: The role of second pass processing., *Journal of Manufacturing Processes* 20(2015) 367-373.
- [21] Ranjit Bauri, et al., Optimized process parameters for fabricating metal particles reinforced 5083 Al composite by friction stir processing., *Data in brief* 5(2015) 309-313.
- [22] H. G. Rana, V. J. Badheka, and A. Kumar., Fabrication of Al7075/B4C Surface Composite by Novel Friction Stir Processing (FSP) and Investigation on Wear Properties., *Procedia Technology* 23(2016) 519-528.
- [23] I. Dinaharan, et al., Microstructure and wear characterization of aluminum matrix composites reinforced with industrial waste fly ash particulates synthesized by friction stir processing., *Materials Characterization* 118(2016) 149-158.
- [24] Yu Chen et al., Effect of initial base metal temper on microstructure and mechanical properties of friction stir processed Al-7B04 alloy., *Materials Science and Engineering: A* 650(2016) 396-403.
- [25] Mansour Rahsepar, and Hamed Jarahimoghdam. "The influence of multipass friction stir processing on the corrosion behavior and mechanical properties of zircon-reinforced Al metal matrix composites., *Materials Science and Engineering: A* 671(2016) 214-220.
- [26] S. Palanivel, et al., A framework for shear driven dissolution of thermally stable particles during friction stir welding and processing., *Materials Science and Engineering: A* 678 (2016) 308-314.
- [27] Vladislav Kulitskiy, et al., Grain refinement in an Al-Mg-Sc alloy: Equal channel angular pressing versus friction-stir processing., *Materials Science and Engineering: A* 674(2016) 480-490.
- [28] Jingyu Han, et al., Influence of processing parameters on the thermal field in Mg–Nd–Zn–Zr alloy during friction stir processing., *Materials & Design* 94(2016) 186-194.
- [29] S. K. Panigrahi Achieving excellent thermal stability and very high activation energy in an ultrafine-grained magnesium silver rare earth alloy prepared by friction stir processing., *Materials Science and Engineering: A* 675 (2016) 338-344.
- [30] Shude Ji, et al., New technique for eliminating keyhole by active-passive filling friction stir repairing., *Materials & Design* 97(2016) 175-182.
- [31] M. A. García-Bernal, et al. Influence of friction stir processing tool design on microstructure and superplastic behavior of Al-Mg alloys., *Materials Science and Engineering: A* 670 (2016) 9-16.
- [32] I. Dinaharan., Influence of ceramic particulate type on microstructure and tensile strength of aluminum matrix composites produced using friction stir processing., *Journal of Asian Ceramic Societies* 4(2)(2016) 209-218.
- [33] Sandeep Kumar Singh, et al., Influence of multi-pass friction stir processing on wear behavior and machinability of an Al-Si hypoeutectic A356 alloy., *Journal of Materials Processing Technology* 236(2016) 252-262.
- [34] Yu Chen, et al., Influence of multi-pass friction stir processing on microstructure and mechanical properties of 7B04-O Al alloy., *transactions of nonferrous metals society of china* 27(4)(2017) 789-796.
- [35] Xizhou Kai, et al., Hot deformation behavior of in situ nano ZrB₂ reinforced 2024Al matrix composite., *Composites Science and Technology* 116(2015) 1-8.
- [36] Yu Chen et al. Influence of multi-pass friction stir processing on the microstructure and mechanical properties of Al-5083 alloy., *Materials Science and Engineering: A* 650(2016) 281-289.